Development 126, 5699-5711 (1999)
Printed in Great Britain © The Company of Biologists Limited 1999
DEV4258

The murine *Bapx1* homeobox gene plays a critical role in embryonic development of the axial skeleton and spleen

Carla Tribioli* and Thomas Lufkin‡

Brookdale Center for Developmental and Molecular Biology, Mount Sinai School of Medicine, One Gustave L. Levy Place, New York, NY 10029-6574, USA

*Present address: Istituto di Genetica Biochimica ed Evoluzionistica, CNR, 27100 Pavia, Italy

‡Author for correspondence (e-mail: Lufkit01@doc.mssm.edu)

Accepted 27 September; published on WWW 24 November 1999

SUMMARY

Our previous studies in both mouse and human identified the *Bapx1* homeobox gene, a member of the *NK* gene family, as one of the earliest markers for prechondrogenic cells that will subsequently undergo mesenchymal condensation, cartilage production and, finally, endochondral bone formation. In addition, *Bapx1* is an early developmental marker for splanchnic mesoderm, consistent with a role in visceral mesoderm specification, a function performed by its homologue *bagpipe*, in *Drosophila*. The human homologue of *Bapx1* has been identified and mapped to 4p16.1, a region containing loci for several skeletal diseases. *Bapx1* null mice are affected by a perinatal lethal skeletal dysplasia and asplenia, with severe malformation or absence of specific bones of the vertebral column and cranial bones of mesodermal origin, with the most severely affected skeletal elements corresponding to ventral structures associated with the notochord. We provide evidence that the failure of the formation of skeletal elements in *Bapx1* null embryos is a consequence of a failure of cartilage development, as demonstrated by downregulation of several molecular markers required for normal chondroblast differentiation (*alpha 1(II) collagen, Fgfr3, Osf2, Indian hedgehog, Sox9*), as well as a chondrocyte-specific *alpha 1 (II) collagen-lacZ* transgene. The cartilage defects are correlated with failed differentiation of the sclerotome at the time when these cells are normally initiating chondrogenesis. Loss of *Bapx1* is accompanied by an increase in apoptotic cell death in affected tissues, although cell cycling rates are unaltered.

Key words: *Bapx1*, Homeobox, Mouse, Axial skeleton, Spleen, Chondrogenesis

INTRODUCTION

During vertebrate development, the initial overt step in axial skeletogenesis is the generation of the paired paraxial mesodermal somites, which are spheres of epithelial cells located on both sides of the neural tube. Positioned immediately ventral to the neural tube is the notochord, which releases local signaling molecules critical for patterning of the ventral somite. Additional inductive signals derived from adjacent lateral plate mesoderm, the dorsal neural tube and surface ectoderm direct the dorsolateral patterning of the somite (reviewed in (Lassar and Munsterberg, 1996; Pourquie et al., 1996). *Sonic hedgehog (Shh)* is a signaling molecule produced by the notochord and its expression coincides with the activation of the transcription factors *Bapx1* and *Pax1* in the ventromedial presclerotome cells of the somite (Borycki et al., 1998; Johnson et al., 1994). *Bapx1* and *Pax1* are the earliest ventral markers for the onset of the somite dorsoventral polarization (Balling et al., 1996; Tribioli et al., 1997). Presclerotome cells subsequently undergo an epithelial-to-mesenchymal transition, migrate ventromedially to surround the notochord and lateral neural tube, and differentiate into chondroblasts. Cells of the chondrogenic lineage produce a cartilaginous matrix (primarily collagen type II) which, in association with proteoglycans, establishes the framework of the fetal skeleton. This framework is subsequently mineralized following chondrocyte hypertrophy and osteoblast differentiation, through the process of endochondral ossification (Cancedda et al., 1995).

The vertebrate skeleton is almost entirely mesodermal in origin, aside from several bones in the skull, which are derived from neural crest (Couly et al., 1993; Noden, 1992) reviewed in (Hanken and Thorogood, 1993). In *Drosophila*, one of the principal genes controlling mesoderm differentiation is the *bagpipe* homeobox gene (Azpiazu and Frasch, 1993; Azpiazu et al., 1996). We have previously isolated from mouse and human, homologues of *bagpipe* termed *Bapx1*. Examination of the expression of *Bapx1* during embryogenesis revealed an expression almost exclusively restricted to paraxial and lateral plate mesoderm, with earliest expression detectable in the presclerotome cells of the somite and in splanchnic mesoderm surrounding the gut endoderm (Tribioli et al., 1997; Tribioli and Lufkin, 1997). During subsequent stages of embryogenesis, *Bapx1* is expressed in essentially all

cartilaginous condensations that will subsequently undergo endochondral ossification and in splanchnic mesoderm-derived tissues giving rise to intestinal smooth muscle, parts of the peritoneal body wall and spleen. To investigate the genetic role of *Bapx1* in embryogenesis, we have undertaken a loss-of-function study. Mice lacking *Bapx1* are asplenic, but have otherwise normal visceral development. Furthermore, *Bapx1* is dispensable for sclerotome migration and early proliferation but is essential for appropriate prechondroblast-to-chondrocyte transition in mesenchymal cells most closely associated with the notochord.

MATERIALS AND METHODS

Construction of the *Bapx1* targeting vector

The targeting vector was constructed from a mouse genomic clone that contains the *Bapx1* gene, which was isolated from a 129/Sv genomic phage library (Tribioli et al., 1997). To construct the targeting vector, a 17 kb genomic *Sal*I fragment was subcloned into pTZ18R (US Biochemicals). A 2.1 kb *Bss*HII fragment encompassing the *Bapx1* exon I-coding region, the single intron and part of exon II-coding sequences, including the homeobox, was deleted (Tribioli and Lufkin, 1997) and replaced by a 1.8 kb *Spe*I fragment that contained the bacterial neomycin resistance gene (neo) selectable marker under the transcriptional control of the phosphoglycerate kinase (PGK) promoter followed by the PGK poly(A) signal. This neo cassette is flanked by two loxP sites (floxed). The PGK neo cassette was cloned in the opposite transcriptional orientation relative to the endogenous *Bapx1* gene and it introduced two new *Sph*I restriction sites into the *Bapx1* allele (Fig. 1A). The targeting vector was linearized at the unique *Xba*I site for electroporation into ES cells.

Generation of recombinant ES cell clones, transgenic and mutant null mice

ES cell transfection, chimera production and testing, and genotyping of offspring are essentially as previous described (Wang et al., 1998). The probe used for the identification of homologous recombinants by Southern blot analysis with *Xba*I+*Sph*I digestion was a 0.5 kb *Hin*dIII-*Xba*I fragment (probe 1, Fig. 1A), containing sequences located distal to the 3′ arm of the homology region present in the targeting vector (Fig.1A). Chimeric male mice from two independent ES clones (two from clone 34 and two from clone 77) were used to transmit the mutant allele, designated *Bapx1neo+*, onto a congenic inbred 129/SvJ background (#000691, The Jackson Laboratory) and an outbred C57BL/6J background. Heterozygotes were intercrossed to obtain homozygous null embryos. Genotyping of embryos obtained from heterozygous crosses was performed by Southern blot analysis (with the probe 1, Fig. 1A) as previously described (Wang et al., 1998).

To generate the *Bapx1neo−* null allele from the *Bapx1neo+* allele, *Bapx1neo+* male heterozygotes were mated with CMV-Cre transgenic female mice, which express Cre recombinase in unfertilized oocytes and preimplantation embryos under the direction of the CMV promoter (Nagy et al., 1998). The resulting offspring were genotyped with *Xba*I+*Sph*I digestion and the *Bapx1* probe1 (Fig. 1B) and with *Bam*HI digestion and a 1 kb *Spe*I fragment as probe from the plasmid pSL13, containing the Cre gene (Li et al., 1997). Heterozygotes with the *neo−* deleted allele, resulting from Cre-mediated recombination, were inbred to produce *Bapx1neo−* null homozygotes (Fig. 1B).

Transgenic mice carrying the *lacZ* reporter under the control of the *mouse pro alpha 1(II) collagen* promoter and enhancer were generated by pronuclear injection of 1-cell B6D2 embryos as previously described (Frasch et al., 1995). The *mouse pro alpha 1(II) collagen-lacZ* (*collagen-lacZ*) transgene construct was kindly provided by Benoit de Crombrugghe and has been previously described (Metsaranta et al., 1995; Zhou et al., 1995). Three transgenic founders showing identical cartilage-specific expression were generated and used for this study. Embryo fixation, β-galactosidase staining and paraffin sectioning was performed as previously described (Frasch et al., 1995; Wang et al., 1998).

RT-PCR assays

RNA was isolated from entire E14.5 mouse embryos and yolk sac DNA was removed for genotyping. Total RNA preparation and first-strand cDNA synthesis were performed as previously described (Tribioli and Lufkin, 1997). The cDNA was then used as a substrate for PCR amplification assays using AMP Taq DNA polymerase (Perkin Elmer) and standard procedures with a final concentration of 10% DMSO in the reaction buffer (Tribioli and Lufkin, 1997). One pair of primers: (o1:5′GAAGAGAACGAGGGCAGGAG 3′ and o2: 5′GCAGTGGCAGAAGGGAAGGTG 3′) was used for the first round of amplification and the pair of primers (o3: 5′CCAAGGACCT-GGAGGAGGAA 3′ and o4: 5′GCAGAGG-CGAGCAGGTCGGC 3′) was used for the nested round. o1 and o3 primers are located in *Bapx1* exon 1, which is deleted in the mutant allele, thus allowing us to distinguish the expression of the wild-type *Bapx1* allele from the *Bapx1* null allele. The specificity of the RT-PCR reactions was verified by Southern blot analysis using the *Bapx1* p1205 plasmid insert as probe. The primers used in the control reactions for β-actin mRNA (antisense: 5′-TCTCCAGGGAGGAAGAGGAT03′; sense: 5′-ATG-TTTGAGACCTTCAACACC-3′) were employed as previously described (Liu et al., 1996).

Histological and skeletal analyses

For histological studies, 7 μm paraffin-embedded sections were collected on glass slides, dewaxed and stained with either: HE, hematoxylin and eosin; or AR, alcian blue and nuclear fast red; or HGF, hematoxylin, fast green and basic fuschin, essentially as described (Sheehan and Hrapchak, 1987). Embryos were fixed in Bouin's solution or in 4% paraformaldehyde overnight (with equivalent results) then dehydrated through graded ethanols, followed by Americlear (substituted for xylene) and paraffin embedding. HE staining was performed essentially as described (Lufkin et al., 1993). AR staining for cartilage was performed on dewaxed and rehydrated sections. Slides were treated for 30 minutes with 1% alcian blue 8GX (Mallinckrodt) in 3% glacial acetic acid, followed by 2 minutes washing in running water and then 5 minutes in nuclear fast red (Kernechtrot) counterstain (Vector Laboratories). Sections were then dehydrated in graded ethanols and coverslipped. HGF staining for collagen-associated proteoglycans was performed as follows. Rehydrated sections were stained in Weigert's iron hematoxylin solution (Sheehan and Hrapchak, 1987) for 1 minute and rinsed with running water until the blue color fully developed. Sections were then transferred to fast green FCF stain (1:5000 aqueous solution) for 3 minutes, rinsed briefly in 1% acetic acid and then stained in 0.1% basic fuchsin (in 1:100 glacial acetic acid:water) for 4 minutes. Sections were then dehydrated in 95% and 100% ethanols and coverslipped. Unless indicated, all stains were obtained from Sigma.

For staining and visualization of whole-mount cartilage and ossified skeletal elements, embryos or neonatal mice were dissected and stained with alizarin red and/or alcian blue, as previously described (Lufkin et al., 1992). For alcian blue/alizarin red combined staining, the skin and internal organs were removed and the samples were fixed overnight in 95% ethanol followed by staining with 0.02% alcian blue in 4:1 95% ethanol:glacial acetic acid for 2 days. The samples were washed in 95% ethanol rapidly and immersed in 2% KOH for several hours to overnight. The samples were then stained in 75 μg/ml alizarin red in 1% KOH overnight, then processed through a graded series of glycerols in ethanol and stored in 100% glycerol. For cartilage staining, E12.5-E14.5 embryos were fixed in Bouin's solution overnight, rinsed rapidly with water several times, immersed in four changes of 1% ammonia in 70% EtOH for at least one hour each and

stained overnight with 0.05% alcian blue in 5% acetic acid. Embryos were rinsed in 5% acetic acid three times for 1-2 hours each and then once overnight. Specimens were dehydrated through graded ethanols, cleared and stored in 2:1 benzyl alcohol:benzyl benzoate (Sigma) and photographed in glass dishes.

RNA in situ hybridization

In situ hybridization analysis was performed as previously described (Tribioli et al., 1997). The following cDNAs were used as templates for synthesizing antisense or sense strand [^{35}S]UTP RNA probes: 0.7 kb *Bapx1* cDNA (p1140) (Tribioli et al., 1997); 0.9 kb BMP4 (Lyons et al., 1989); 0.4 kb *Fgfr3* (Goldfarb, 1990); 3.0 kb *Mfh1* (Winnier et al., 1997); 1.5 kb *Shh* (Echelard et al., 1993); 0. 473 kb *pro alpha1(II) collagen* (Andrikopoulos et al., 1992); 0.313 kb *Pax1* (Koseki et al., 1993); 0.270 kb *Osf2* (pLA-Oa4) (Ducy et al., 1997); 1.8 kb *Ihh* (Yang et al., 1998); To distinguish the expression of the *Bapx1* wild-type allele from the two null alleles, we employed the *Bapx1 probe2* (pGIA115), which contains *Bapx1* cDNA sequences from nt 268 to nt 687 (Tribioli et al., 1997), which are deleted in the *Bapx1*neo+ and *Bapx1*neo– mutant alleles.

Cell proliferation and apoptosis

To determine cell proliferation, DNA synthesis was examined by measuring 5-bromo-2′-deoxyuridine (BrdU) incorporation into cells of E10.5-E14.5 embryos. Pregnant mice were injected intraperitoneally with a mixture of BrdU (Sigma B-9285) and 5-fluorodeoxyuridine (FUdr, Sigma F-0503) at 50 μg and 10 μg per gram body weight, respectively. After 1 hour, the embryos were removed, fixed in 4% paraformaldehyde overnight at 4°C, dehydrated in a graded ethanol series and embedded in paraffin. 7 μm sections

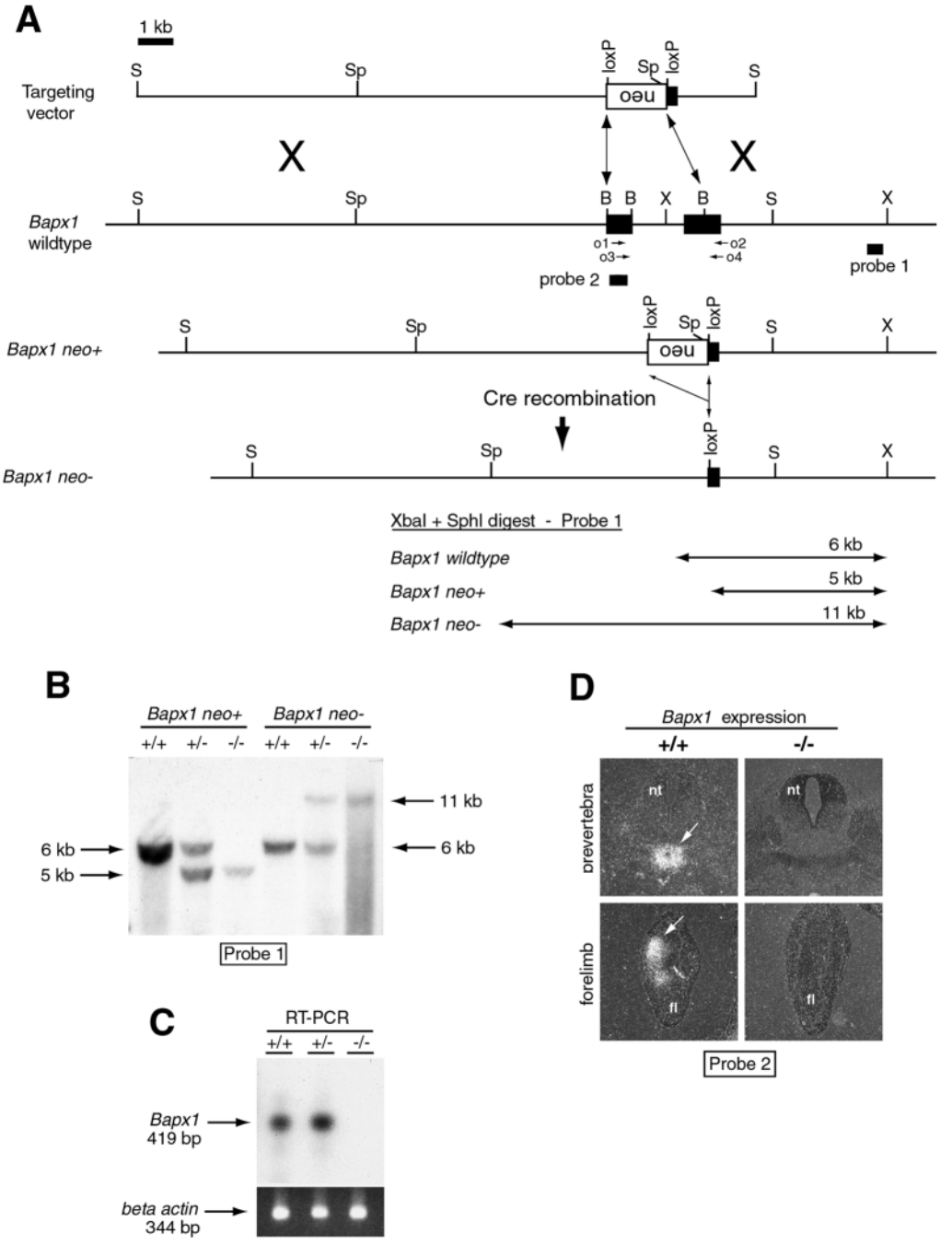

Fig. 1. Disruption of the *Bapx1* gene and loss of *Bapx1* expression. (A) The structure and a partial restriction map of the targeting vector, the wild-type genomic *Bapx1* locus and the mutated allele before and after the deletion of the neomycin-resistance gene (neo) gene are shown. The exons and the neo are shown as black and white boxes, respectively. Restriction enzymes are: B, *Bss*HII; H, *Hin*dIII; S, *Sal*I; Sp, *Sph*I; and X, *Xba*I. Only pertinent restriction sites are depicted for some of the indicated restriction enzymes. The localization of probe 1 used for Southern blotting and the size of the expected *Xba*I+*Sph*I diagnostic fragments are shown. The location and orientation of o1, o2, o3, o4 primers for RT-PCR is indicated. The position of the probe for RNA in situ analysis (probe 2) is indicated. (B) Southern blot analysis of *Bapx1* offspring. Bands are indicated which correspond to wild type (6 kb) and mutant *Bapx1* genes with neo (5 kb) or without neo (11 kb) after Cre-mediated recombination. (C) Southern blot of the nested RT-PCR products of *Bapx1* gene (419 bp) utilizing two pairs of oligonucleotides (o1 and o2; o3 and o4). Agarose-gel electrophoresis of ethidium bromide-stained cDNA products from RT-PCR of mRNAs for β-actin (344 bp) was used to normalize for the amount of mRNA used. (D) In situ hybridization on sections using antisense ^{35}S-labeled probe 2 riboprobe in wild type (+/+) and null (–/–) embryos at E12.5 is shown. Arrows indicate expression in prevertebrae and forelimb in wild-type embryos. No expression of *Bapx1* was detected in *Bapx1* null embryos.

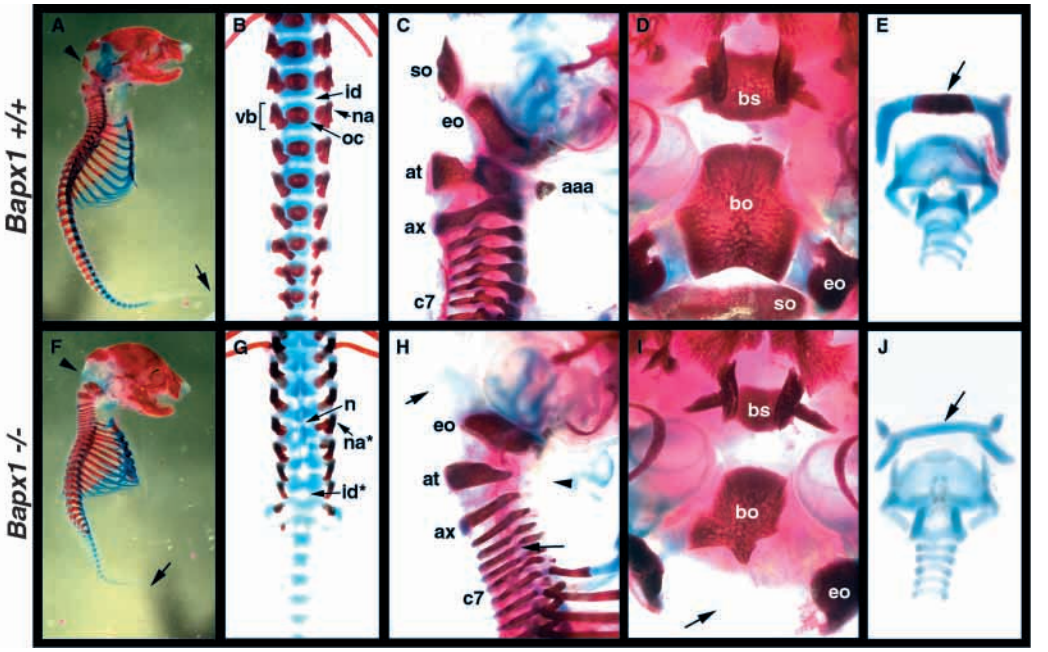

Fig. 2. Bone and cartilage staining of E18.5 embryos performed with alcian blue and alizarin red. (A-E) *Bapx1* wild type; (F-J) *Bapx1* null. (A,F) Lateral view of fetal skeleton. The appendicular skeleton (limbs) which was unaffected has been removed. The tip of the tail is indicated with an arrow. The position of the supraoccipital bone (missing in F) is indicated with an arrowhead. Note the overall length of the axial skeleton is dramatically reduced in the *Bapx1* null offspring although the total number of vertebrae is the same. (B,G) Enlarged view of the lumbar region. Note the absence of ossification centers (oc) in the vertebral bodies (vb) of the *Bapx1* null skeletons, and the neural arches (na) are also reduced in size. Absence of the ventral portion of the vertebral body exposes the notochordal remnant (n) in the *Bapx1* null animals. (C,H) Close up of the cervical region showing the missing supraoccipital bone (so, arrow) and anterior arch of atlas (aaa, arrowhead). Fissures in the neural arches are evident (H, long arrow) as well as an overall reduction in arch width and compression of the vertebral column. (D,I) Ventral view of the skull showing dysmorphologies of the basisphenoid (bs), basioccipital (bo), exoccipital (eo) and complete absence of the supraoccipital (so, arrow). (E,J) Frontal enlarged view of ossification center (arrows, missing in J) of the cartilage primordium of the body of the hyoid bone. Thyroid and cricoid cartilages, which appear normal, are visible below. Abbreviations: aaa, anterior arch of atlas; at, Atlas (C1); ax, Axis (C2); bo, basioccipital; bs, basisphenoid; eo, exoccipital; id, intervertebral disk; n, notochord remnant; na, neural arch; oc, ossification center of vertebral body; so; supraoccipital; vb, vertebral body.

were cut and mounted on glass slides then dewaxed in Americlear and rehydrated through a graded series of ethanols with water as a final wash. BrdU-positive cells were identified using a mouse monoclonal antibody (clone BMC 9318, IgG1) followed by a sheep anti-mouse Ig-alkaline phosphatase and NBT/X-phosphate color reaction essentially as described by the supplier (Boehringer Mannheim). Antibody incubations were performed for 1 hour at 37°C in a humidified incubator and all washes were performed at room temperature. Following the AP color reaction at room temperature for 10-20 minutes, slides were washed three times in PBS and then coverslipped in DTG2; 2.5% DABCO, 17.5% 0.5 M Tris pH 8.6, 80% glycerol, the edges sealed with nail hardener and stored at 4°C. Following photography, cells of the prevertebrae were scored as labeled or unlabeled in ten or more sections from at least two independent embryo preparations and cells of the overlying neural tube or adjacent lateral plate mesoderm were scored for an internal control.

Apoptotic cell death was examined by analyzing the extent of oligonucleosomal DNA cleavage (TUNEL) in cells of E10.5-E14.5 embryos. *Bapx1* wild-type and null embryos derived from *Bapx1* heterozygote intermatings were genotyped, fixed, paraffin embedded and sectioned as described above. Dewaxed and rehydrated sections were incubated in permeabilisation solution (0.1% Triton X-100 in 0.1% sodium citrate) for 8 minutes, rinsed three times in PBS and incubated with terminal deoxynucleotide transferase (TdT) and fluorescein-conjugated dUTP for 1 hour at 37°C as described by the supplier (Boehringer Mannheim). Slides were washed three times in PBS at room temperature and the incorporated fluorescein-dUTP was detected using an alkaline phosphatase-labeled anti-fluorescein antibody followed by NBT/X-phosphate color reaction. Section washing, coverslipping, photography and cell counting are as described above.

RESULTS

Targeted disruption of the murine *Bapx1* gene

Because the *Bapx1* deleted region comprises nearly all of the coding region and the *neo* substitution introduces multiple stop codons into *Bapx1* exon II, the disruption would be predicted to result in a null allele. This allele is referred to as *Bapx1neo+*. The linearized targeting vector was electroporated into ES cells and clones were selected for resistance to G418. 80 resistant clones were analyzed by Southern blotting using a 3′ probe (probe1) external to the targeting vector, and 8 independent cell lines, including clone 34 and clone 77, yielded the 5 kb *Xba*I+*Sph*I band expected from a homologous recombination event (Fig. 1A), giving an overall frequency of 10%. ES clones 34 and 77 were injected into C57BL/6J blastocysts to generate chimeras that transmitted the *Bapx1* null allele to their progeny. The *Bapx1* null allele was either outcrossed to the C57BL/6J strain or maintained on a congenic inbred 129/SvJ background. Heterozygous mice were identified by Southern blot analysis of tail genomic DNA, and were viable, fertile, healthy and born in appropriate Mendelian ratios. However, careful examination of skeletal preparations of E18.5 $Bapx1^{-/+}$ embryos revealed, in 78% of the individuals examined, mild abnormalities of the vertebrae, such as split or reduced ossification centers, which did not affect the overall length of the vertebral column nor the morphology of the neural arches. These defects were observed primarily in the lumbar vertebrae. This indicates that *Bapx1* is haploinsufficient in some axial skeletal elements.

Using CMV-Cre transgenic mice (Nagy et al., 1998), Cre-

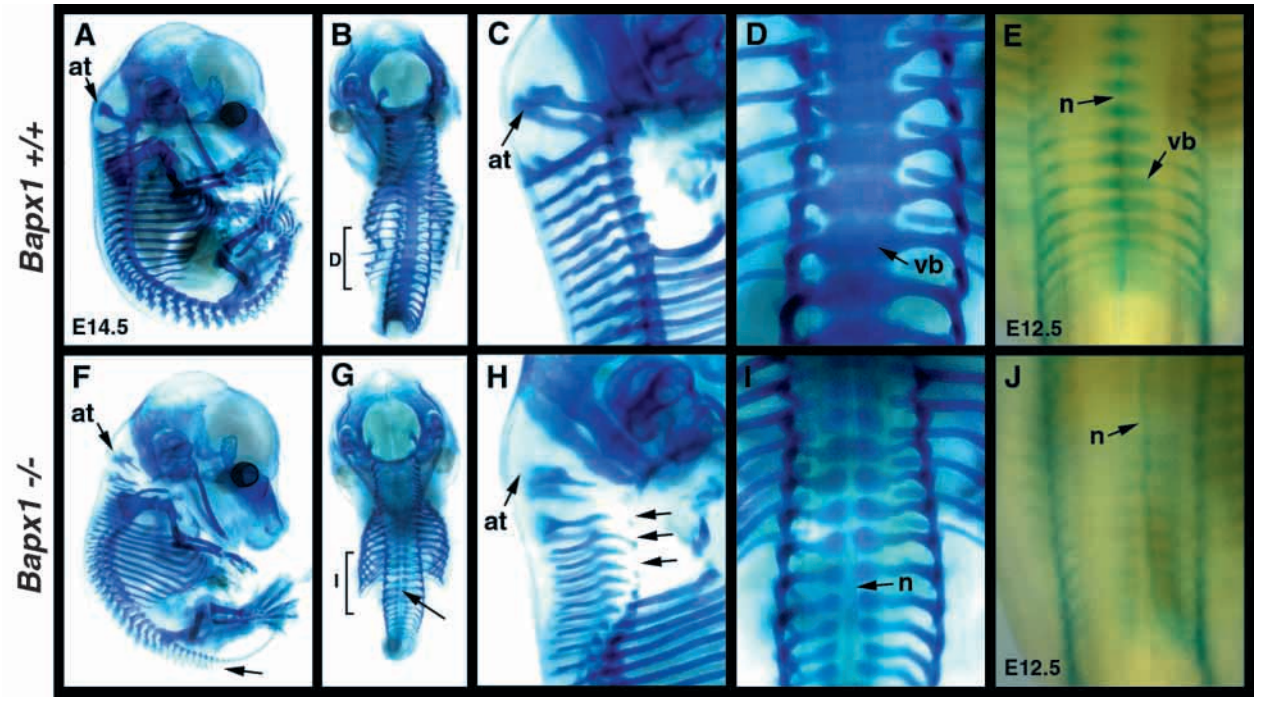

Fig. 3. Cartilage staining of E12.5 and E14.5 embryos. (A-E) *Bapx1* wild type; (F-J) *Bapx1* null. (A-D,F-I) E14.5; (E,J) E12.5. (A,F) Lateral view of the cartilaginous skeleton. The arrow in F indicates that dramatically reduced axial skeleton and the faulty chondrogenesis of the vertebrae. (B,G) Dorsal view of embryos showing the impaired chondrogenesis which is most pronounced in the midline (arrow in G). The lumbar regions detailed in D,I are marked with brackets. (C,H) Lateral enlarged view of the cervical region. Failed chondrogenesis of the vertebral bodies of the cervical region is indicated with arrows. (D,I) Dorsal close up of the regions outlined in B,G. The absence of chondrogenesis in the vertebral bodies is evident and the notochord is almost entirely exposed. Note also the compressed spacing between adjacent vertebral bodies. (E,J) Dorsal view of an E12.5 embryo showing identical defects observed at later stages of development, indicating that the *Bapx1* function is necessary prior to E12.5. Abbreviations: at, Atlas (C1); n, notochord; vb, vertebral body.

Table 1. Offspring from *Bapx1neo*+ heterozygote crosses

Age	Litters	+/+ (%)	+/– (%)	–/– (%)
E10.5	12	28 (30)	44 (48)	20 (22)
E12.5	14	36 (30)	56 (47)	28 (23)
E14.5	10	18 (24)	37 (50)	19 (26)
E18.5	7	8 (19)	23 (55)	11 (26)
Newborn	8	11 (19)	30 (53)	16 (28)

Table 2. Summary of skeletal defects observed in *Bapx1*$^{-/-}$ mutant mice

Structure	Defect	Mesodermal origin
Basisphenoid	malformed	cephalic MPM
Supraoccipital	absent	cephalic MPM
Exoccipital	reduced	somitic
Basioccipital	malformed	somitic
Anterior arch of atlas	absent	somitic
Vertebral body (ventral)	absent	somitic
Neural arches	reduced	somitic
Intervertebral disc	reduced	somitic

Cephalic MPM, cephalic medial paraxial mesoderm (Couly et al., 1992, 1993).

mediated recombination of the *Bapx1neo*+ allele in vivo excised the inserted "floxed" PGKneo gene. Thus, heterozygous mice carrying a null mutant *Bapx1neo*– allele were established as an independent line and were interbred to produce mutant homozygotes. Analysis of homozygous mutant embryos from *Bapx1* null heterozygous crosses at various developmental stages (E10.5-18.5) revealed that they were present in appropriate Mendelian ratios indicating that there was no significant embryonic lethality (Table 1). We observed an identical phenotype in *Bapx1neo*– homozygous and in *Bapx1neo*+ homozygous mice, suggesting that the mutant phenotype results from the loss of *Bapx1* and not from the influence of PGKneo on other sequences. To ensure that *Bapx1* was not expressed as a functional protein, we carried out RT-PCR assays with RNA extracted from homozygous *Bapx1neo*+ mutant and from wild-type mouse embryos. Homozygous mutant embryos lacked an amplified *Bapx1* cDNA from the region spanning the *Bapx1*-coding sequences deleted in the mutant allele (Fig. 1C). In further confirmation of the functional disruption of the *Bapx1* gene, RNA in situ hybridization on mouse embryo sections with the GIA115 riboprobe (probe 2, Fig. 1A) which is deleted in the *Bapx1* null alleles, showed that no *Bapx1* transcript was present in the homozygous *Bapx1neo*+ mutant embryos in two primary sites of *Bapx1* expression: the sclerotome (prevertebrae) and the forelimb (Fig. 1D).

Disruption of *Bapx1* gene results in perinatal recessive lethality

Analysis of the genotype of 10-day-old pups from numerous *Bapx1* heterozygous mutant intercrosses did not reveal any

Bapx1 null offspring. To characterize the time point of lethality in *Bapx1* null mice, yolk sac or tail DNA from mice at various developmental stages (E10.5-18.5) and from newborn mice (either naturally born or from Cesarean delivery) was analyzed (Fig. 1B). The results (Table 1) suggested that *Bapx1* null fetuses were not subject to prenatal lethality; however, we noticed that newborn *Bapx1* null mice died within minutes of birth, probably as a result of failing to initiate normal respiration. Superficial examination of the *Bapx1* null pups, revealed overall similarity in body weight relative to wild-type and heterozygous littermates but the *Bapx1* null pups had severely truncated tails and appeared slightly shorter in stature and displayed a clearly distended circumference of the thoracic and abdominal areas (barrel chest appearance). Since no *Bapx1* null pups survived birth, we concluded that loss of *Bapx1* resulted in a recessive perinatal lethal phenotype. Identical phenotypes were obtained with mouse lines generated from each of the two independent ES clones 34 and 77 and in both C57BL/6J mixed and 129/SvJ inbred backgrounds and with *neo* present or following removal with Cre recombinase.

Cartilage and bone defects in *Bapx1* null embryos

Anatomical examination and alcian blue/alizarin red staining of cartilage and bone at different stages of chondrogenesis and mineralization (E12.5-E18.5) revealed a dramatically hypoplastic axial skeleton in the *Bapx1* null embryos (Figs 2A,F, 3A,F). The reduction in length of the vertebral column appears to be primarily the result of a reduction in the overall rostrocaudal length of the individual vertebrae. The total number of vertebrae appears approximately normal in the *Bapx1* null embryos but, in all vertebrae, the vertebral bodies (vb) were hypoplastic, with only a small region of the dorsal vertebral body still present and with the complete absence of the ventral vertebral body. In all of the vertebral bodies at E18.5, we observed a total loss of ossification centers (oc, Fig. 2B,G), which was preceded, beginning at E12.5, with similar defects in chondrogenic condensations surrounding the notochord (Fig. 3). In addition, the neural arches (na) and intervertebral discs (id) were approximately 0.2-0.5 times the normal thickness and the notochordal remnant (n) was left exposed (Figs 2, 3). The ribs appeared normal but the thoracic cavity was distended radially. In the occipital and cervical region, the neural arches were reduced in size and displayed fissures (long arrow, Fig. 2). This defect was also observed for the exoccipital bone (eo, Fig. 2), which is the occipital equivalent of a neural arch. The anterior arch of atlas (aaa, Fig. 2) was completely absent. The floor of the cranial vault was highly affected in the *Bapx1* null embryos, with either a reduction in size or a severe dysmorphology of the basisphenoid (bs) and basioccipital bones (bo, Fig. 2D,I). Note also the complete loss of the supraoccipital bone (so in Fig. 2C,H) as well as the total absence of the ossification center of the cartilage primordium of the body of the hyoid bone (arrows Fig. 2E,J, missing in *Bapx1*$^{-/-}$). Because *Bapx1* null embryos at E12.5 and E14.5 displayed identical defects in chondrogenesis of the axial skeleton (Fig. 3E,J) as were observed at later stages of fetal development, we concluded that the function of *Bapx1* in chondrogenesis is required prior to E12.5. Interestingly, no skeletal defect was observed in the limbs at any stage (e.g. Fig. 3) despite that significant *Bapx1* expression has been detected there (Tribioli et al., 1997; Tribioli and Lufkin, 1997).

Histological and immunohistochemical analysis of skeletal and spleen defects in *Bapx1 null* mutants

Histological examination of *Bapx1* wild-type and null embryos at E12.5 and earlier stages, however, showed no alterations in the number or density of cells surrounding the notochord (Fig. 4A,B) suggesting that the defects in the *Bapx1* null embryos are less related to cell migration than to cell differentiation. Cartilage production and chondroblast differentiation was examined in *Bapx1* wild-type and null embryos using AR (alcian blue and nuclear fast red) or HGF (hematoxylin, fast green, and basic fuschin) staining, which are indicators of cartilage and collagen-associated proteoglycan (primarily aggrecan) production, respectively. Examination of the vertebral bodies (vb) in *Bapx1* null embryos revealed complete agenesis of the ventral portion of the vertebral body (Fig. 4C-H) and faulty differentiation of the cells of the dorsal vertebral body, with the most affected cells positioned in closest association with the notochord (arrows, Fig. 4E-H). The mechanism for the agenesis and failed chondrogenesis of the vertebral bodies was investigate by analyzing *Bapx1* wild-type and null embryos for alterations in cell proliferation and cellular apoptosis (Fig. 4I-L). To determine cell proliferation, DNA synthesis was examined by measuring 5-bromo-2′-deoxy-uridine (BrdU) incorporation into cells of *Bapx1* wild-type and null embryos between the ages of E10.5 and E14.5. The results from this assay (Fig. 4K,L) showed no significant differences in the cell proliferation rates in the cells of the sclerotome/vertebral body or in adjacent tissues at any stage examined. In contrast, when apoptotic cell death was examined by analyzing the extent of oligonucleosomal DNA cleavage (TUNEL) in cells of *Bapx1* wild-type and null embryos, a 2.7-fold increase in the number of cells undergoing apoptosis was observed in the developing vertebral bodies of the *Bapx1* null embryos, whereas no alterations in apoptosis rates were observed in adjacent tissues of these same embryos (Fig. 4I,J). Another significant domain of expression of *Bapx1* in the developing embryo is the lateral plate mesoderm surrounding the midgut (Tribioli et al., 1997). *Bapx1* wild-type and null embryos were examined for alterations in midgut development and morphology. Surprisingly, no obvious defects in smooth muscle development were observed in the *Bapx1* null embryos (Fig. 4M,N). In contrast, the *Bapx1* null newborns displayed fully penetrant asplenia (Fig. 4O,P). Examination of earlier stage embryos (E11.5-E16.5) showed that the earliest absence of spleen precursor cells in the *Bapx1* null embryos coincided with the timing of the normal appearance of the spleen anlage in wild-type embryos (E11.5), which is derived from a condensation of coelomic epithelium and underlying mesenchyme of the dorsal mesogastrium (Green, 1967), both cells types that normally express *Bapx1* (Tribioli et al., 1997).

Molecular analysis of *Bapx1* null mutants

Histological analysis of the *Bapx1* null embryos suggested a defect in both growth and differentiation of the chondrogenic regions of the axial skeleton, particularly those regions that would subsequently undergo endochondral ossification. To extend this analysis and to investigate with molecular markers

the *Bapx1* null phenotype, we generated transgenic lines that drive expression of β-galactosidase in cartilaginous condensations and mature cartilage using the regulatory elements from the *mouse pro alpha 1(II) collagen* gene which has been shown to confer restricted expression to nearly all cartilaginous condensations in the developing embryo (Metsaranta et al., 1995; Zhou et al., 1995). β-galactosidase staining of *Bapx1* wild-type and null embryos carrying the *mouse pro alpha 1(II) collagen-lacZ* transgene revealed an altered *lacZ* expression pattern in the axial skeleton, which is most evident in whole-mount-stained embryos in the tail region (Fig. 5A,B,E,F). In wild-type embryos, the *mouse pro alpha 1(II) collagen-lacZ* transgene shows clearly defined segmental expression in the developing vertebrae, which is absent in the *Bapx1* null embryos (Fig. 5C,H). Transverse sections of the vertebral column in *Bapx1* null embryos with the *mouse pro alpha 1(II) collagen-lacZ* transgene revealed a complete absence of β-galactosidase activity in the cells surrounding the notochord (n, Fig. 5I) which in wild-type embryos show strong β-galactosidase expression and which will subsequently form the vertebral body (vb, Fig. 5D).

Many transcription factors, signaling molecules and extracellular matrix molecules have been shown to play a critical role in normal development of the fetal skeleton. *alpha 1(II) collagen (Col2a1)* is one of the earliest markers for cells entering the chondroblast lineage (Aubin et al., 1995; Cancedda et al., 1995). The expression of *alpha 1(II) collagen* was downregulated in the ventral vertebral bodies of *Bapx1* null embryos (Fig. 6A,B,E,F) and the expression of *alpha 1(II) collagen* in other regions of the axial skeleton showed a reduced expression pattern similar to the AR and HGF histological staining results for chondrogenic regions (described above, Fig. 4). The runt domain-containing transcription factor *Osf2/Cbfa1* which is expressed in a common progenitor for chondroblasts and osteoblasts and is required for differentiation of the later (Ducy et al., 1997) was also downregulated in the *Bapx1* null embryos (Fig. 6M,N,Q,R). This result was not surprising given the complete absence of vertebral body ossification in the *Bapx1* null embryos. In a similar manner, expression of the cell-cell signaling molecule *Indian hedgehog (Ihh)* which is expressed in prehypertrophic chondrocytes and is a regulator of the passage of cells from the proliferative to prehypertrophic chondrocyte stage, was dramatically reduced in the *Bapx1* null embryos (Fig. 6C,D). The transcription factors *Pax1* and *Mfh1* are absolutely required for proper differentiation of the sclerotome and, in particular, for the formation of the vertebral bodies (Iida et al., 1997; Wilm et al., 1998; Winnier et al., 1997). In addition, both genes have been shown to be induced by *Shh* signals from the notochord (Furumoto et al., 1999). Both *Pax1* and *Mfh1* are expressed at normal levels in *Bapx1* null embryos; however, both genes showed slightly altered patterns of transcript distribution in the vertebral bodies (Fig. 6G-J), and this alteration appears related to the histological disruption of the vertebral body tissue, rather than to a regulatory effect. The zinc-finger transcription factor *Gli2* and the cell-cell signaling molecule *sonic hedgehog (Shh)*, both of which play a positive regulatory role in the induction of the sclerotome and normal skeletal development, are unaffected in the *Bapx1* null background (Fig. 6K,L,O,P). The third fibroblast growth factor receptor, *Fgfr3*, which negatively regulates osteogenesis by inhibiting chondrocyte proliferation and differentiation shows widespread expression throughout the prevertebrae of E12.5 wild-type embryos; however, expression of *Fgfr3* is absent from the prevertebrae of *Bapx1* null embryos (Fig. 6U,V). The expression of bone morphogenetic protein 4, *Bmp4*, which is a regulator of somite differentiation, and is under the negative feedback control of *Ihh* (Aubin et al., 1995; Vortkamp et al., 1998) is normally restricted to the perichondrial region of E12.5 wild-type embryos. In the *Bapx1* null embryos, *Bmp4* expression is observed throughout all of the cells of the prevertebrae and is no longer restricted to the perichondrial region (Fig. 6W,X). *Sox9* is normally expressed throughout all cartilaginous condensations of the developing preskeleton (Ng et al., 1997; Wright et al., 1995; Zhao et al., 1997) and has been shown to be absolutely required for cartilage formation in loss-of-function studies (Bi et al., 1999) and to be a direct regulator of *alpha 1(II) collagen* expression (Bell et al., 1997; Healy et al., 1999; Lefebvre et al., 1997; Ng et al., 1997). A decrease in *Sox9* expression is observed in *Bapx1* null embryos, in mesenchymal cells migrating to form the sclerotome surrounding the notochord, the precursor of the vertebral body (Fig. 6Y,Z). During subsequent development, *Sox9* is downregulated in the ventral prevertebral body and in prechondrogenic cells surrounding the notochord (n, Fig. 6AA,BB). A probe specific to the 3′ end of the *Bapx1* gene, which is still present in the *Bapx1* null mutation, showed normal cell distributions and cell densities for the population of prevertebral cells expressing the *Bapx1* null allele at E12.5 (Fig. 6S,T). Taken together, our results suggest that the developmental function of *Bapx1* is dispensable for sclerotome migration and proliferation but is required for directing ventral sclerotomal cells towards a chondroblast pathway, and this effect is most pronounced in cells in closest apposition to the notochord. An increase in the rate of programmed cell death may account in part for the loss of tissue in the *Bapx1* null embryos.

DISCUSSION

Bapx1 function during embryonic development of the skeleton and spleen

The *Bapx1* null embryos die perinatally and show a dramatically reduced and unossified axial skeleton and asplenia. The absence of spleen precursor cells is observed from the earliest stages of initiation of the splenic anlage from lateral plate mesoderm. The absence of ossification centers in the ventral axial skeletal elements in *Bapx1* null newborns is preceded at earlier stages by failed chondrogenesis of the same tissues. Since endochondral ossification proceeds upon a cartilaginous outline, the absence of ossification in the *Bapx1* null offspring is likely related to earlier defects in chondrogenesis, although a direct effect upon a chondro/osteoblast precursor cannot be ruled out. The analysis of prechondrogenic cells (E10.5-12.5) of the embryonic axial skeleton in *Bapx1* wild-type and null embryos showed no significant differences in cell migration patterns or cell density and the overall morphology of the prechondrogenic prevertebrae appeared identical. In addition, identifying cells that normally express *Bapx1* with a RNA in situ probe against

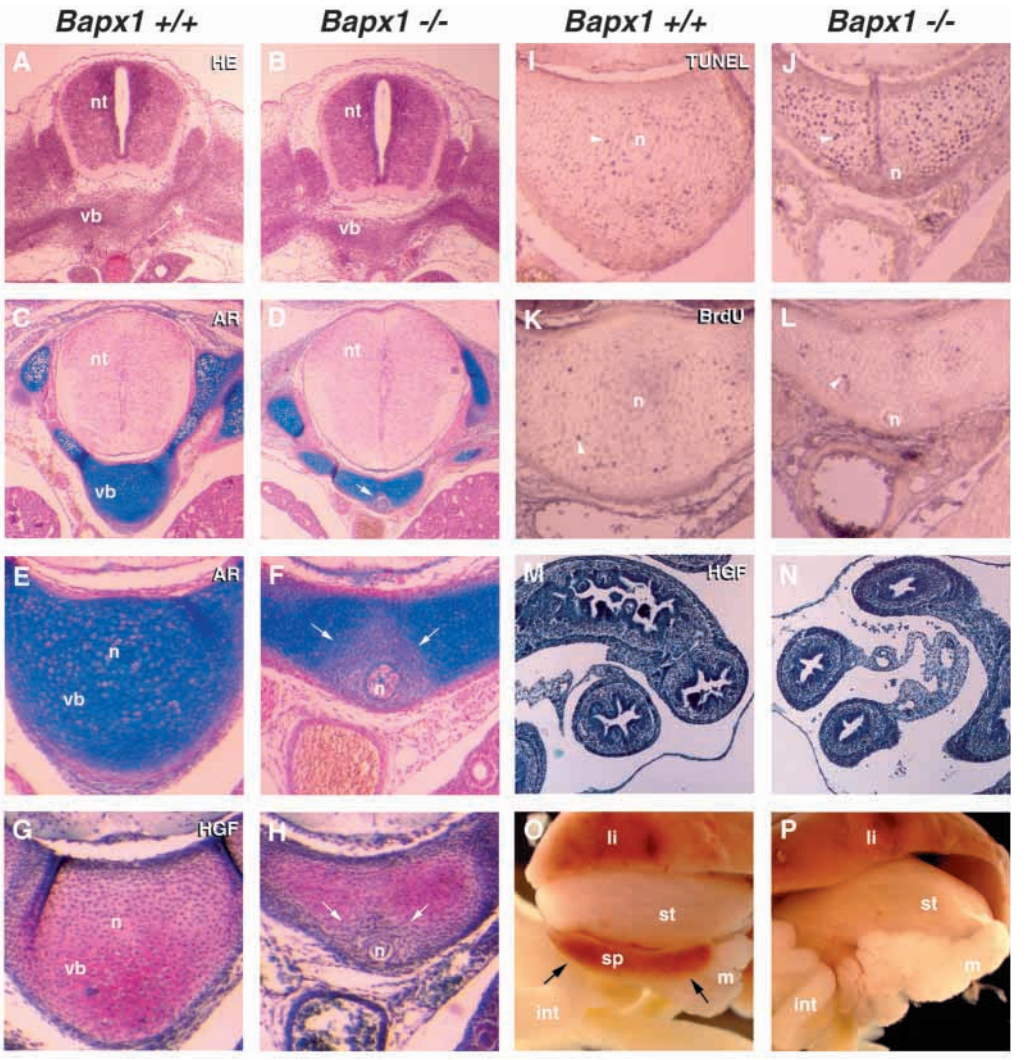

Fig. 4. Histological and immunohistochemical analysis of the *Bapx1* vertebral column and midgut. The *Bapx1* genotype is indicated above each column. All sections are from E14.5 embryos except A,B which are E12.5. (A-L) Transverse sections through the thoracic region; (M-N) transverse sections through the midgut. The histological procedure is indicated in the upper righthand corner of the *Bapx1*$^{+/+}$ panel. (A,B) In E12.5 embryos, no overt histological alterations are observed in cell density or cell number in the region of the prevertebral body. (C,D) Alcian blue and nuclear fast red (AR) staining of cartilage show dramatically decreased cell numbers in the vertebral body and faulty differentiation of chondroblasts. (E,F) Enlarged view of the vertebral body (vb) stained with AR, showing cells absent primarily from the ventral portion of the vb (ventral to the notochord, n) and faulty differentiation of cells in closest proximity to the notochord as indicated with arrows. (G,H) Enlarged view of a vertebral body stained with HGF for cartilage-specific collagen-associated pericellular secreted proteoglycans (mucins), which appear red after staining. Absence of the ventral vertebral body and an area of undifferentiated cells surrounding the notochord are evident (arrows). (I,J) Analysis of apoptotic cell death by analyzing the extent of oligonucleosomal DNA cleavage (TUNEL) in cells of the vertebral body. An increased density of cells undergoing apoptosis (arrowheads) is observed in the remnant of the vertebral body in the *Bapx1* null embryos. (K,L) Cell proliferation was assayed by measuring DNA synthesis based upon 5-bromo-2′-deoxy-uridine (BrdU) incorporation into cells of midgestation embryos (arrowheads). No significant difference in the percentage of cycling cells was observed between the two genotypes. (M,N) Histological analysis of transverse sections of the midgut. No visible differences were observed in smooth muscle differentiation in the *Bapx1* null embryos. (O,P) Whole-mount paraformaldehyde-fixed internal organs from E18.5 embryos. Complete asplenia is observed in *Bapx1* null embryos. The spleen (sp) in a wild-type *Bapx1* embryo is indicated with black arrows in O. Abbreviations: AR, alcian blue and nuclear fast red staining; BrdU, cell proliferation assay; HE, hematoxylin and eosin staining; HGF, hematoxylin, fast green and basic fuschin staining; int, intestine; li, liver; m, fatty mesentery; n, notochord; sp, spleen; st, stomach; TUNEL, apoptosis assay; vb, vertebral body.

mRNA sequences that are still present in the *Bapx1* null mutation, showed normal cell distributions and densities for the population of *Bapx1*$^{-/-}$-expressing cells, suggesting that *Bapx* function is dispensable for sclerotome migration and early proliferation, but is required for some later step in skeletal development. Cartilage is the primary product of chondroblasts and is composed of two principal types of molecules, alpha 1 (II) collagen fibrils and proteoglycans. During subsequent stages of development, the cells of the vertebral body fail to differentiate into chondroblasts as assayed by alcian blue (AR) staining (specific for cartilage) or fuschin (HGF) staining (specific for proteoglycans), or when assayed for *alpha 1 (II) collagen (Col2a1)* mRNA expression. Furthermore, using a cartilage-specific *mouse pro alpha 1 (II) collagen-lacZ* transgene as a marker, we observed a loss of β-galactosidase expression in the vertebral bodies of *Bapx1* null embryos, but not in wild-type embryos. Hence the cells of the prevertebrae in the *Bapx1* mutants appear to fail to make the prechondroblast-to-chondrocyte transition. No significant differences were observed in the cell proliferation rates in the axial skeleton between *Bapx1* wild-type and null embryos; however, an increase in the number of cells undergoing apoptosis was observed in the *Bapx1* null prevertebrae. An increase in the rate of programmed cell death may account in part, for the loss of tissue in the *Bapx1* null skeleton. An increase in apoptosis in cells that are unable to complete their normal developmental pathway has been observed in other systems (D'Mello, 1998; Milligan and Schwartz, 1997; Sanders and Wride, 1995) and, in particular, for certain developmental pathways involving homeobox-containing genes (Tiret et al., 1998).

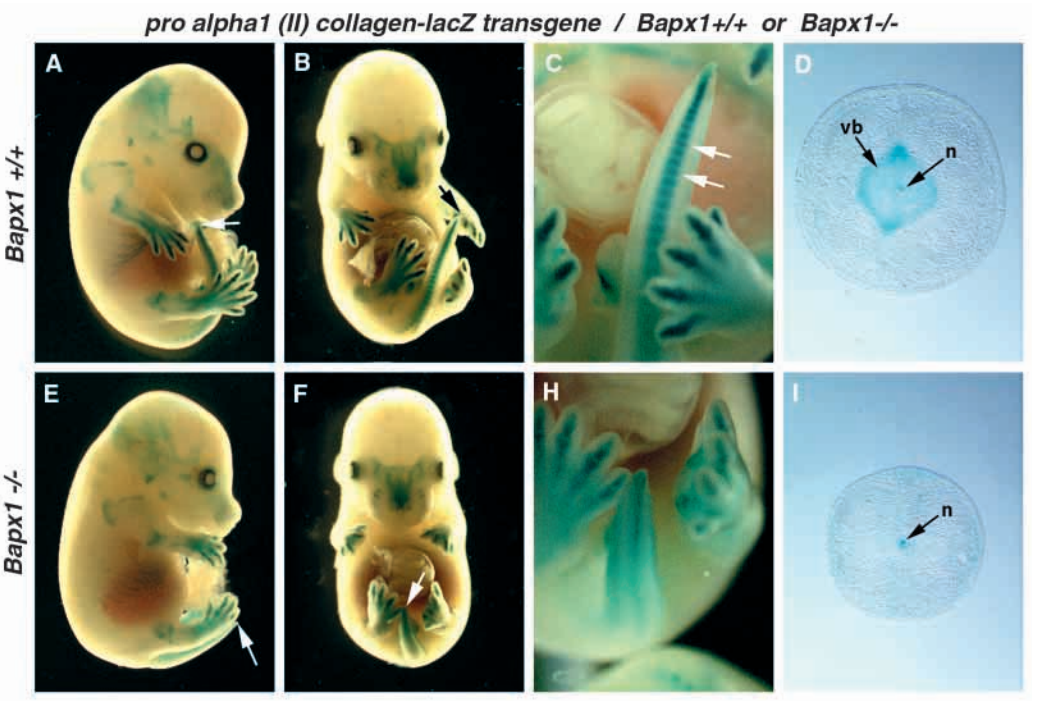

Fig. 5. Expression of the cartilage-specific *mouse pro alpha 1(II) collagen-lacZ* transgene in *Bapx1* wild-type and null backgrounds. The *Bapx1* genotype is shown to the left of each row. (A,E) Lateral view of E14.5 β-galactosidase-stained embryos. The tip of the tail is indicated with an arrow. (B,F) Ventral view of the embryos shown in A,E. Note the truncation of the tail (arrows) and the diffuse β-galactosidase staining in the vertebral column of the *Bapx1* null embryo. (C,H) High-magnification view of the tails. Note the staining of the evenly space vertebral bodies (arrows) in the *Bapx1*$^{+/+}$ embryo which are absent in the *Bapx1* null embryo. (D,I) Transverse sections through the base of the tails of E14.5 β-galactosidase-stained embryos. Note the overall reduction in circumference of the *Bapx1* null tail and the absence of any β-galactosidase staining in the area of the vertebral body (vb) which is centered around the notochord (n).

The role of *Bapx1* in the developmental program of skeletogenic genes

Osf2/Cbfa1 is a runt domain-containing transcription factor strongly expressed in all mesenchymal condensations of the E12.5-E14.5 skeleton in a common progenitor for chondroblasts and osteoblasts. Later in development *Osf2* is expressed primarily in cells of the osteoblast lineage and not in differentiated chondrocytes (Ducy et al., 1997; Komori et al., 1997; Otto et al., 1997). Analysis of *Osf2* in *Bapx1* null embryos showed that its expression was downregulated in the axial skeleton. No alteration in *Osf2* expression was observed in other regions, such as the limbs, which co-express *Bapx1*, but interestingly show no defects in the *Bapx1* null mice. It remains to be determined whether *Bapx1* is a regulator of *Osf2* expression in a common chondro/osteoblast progenitor, or whether loss of *Osf2* expression in these affected *Bapx1* null cells results as a secondary effect of their inability to complete their normal developmental program. *Ihh* is expressed in prehypertrophic chondrocytes and has been shown to regulate the rate of chondrocyte differentiation by stimulating parathyroid hormone-related protein (PTHrP) expression in the adjacent perichondrium. This in turn inhibits the transition from proliferating to prehypertrophic chondrocytes in the internal chondrogenic region (Lanske et al., 1996; Vortkamp et al., 1996). While *Ihh* showed strong expression in the caudal vertebrae of wild-type embryos, no expression of *Ihh* was detected in the caudal vertebrae of *Bapx1* null embryos. This effect was restricted to the axial skeleton, as there was no effect of *Bapx1* on *Ihh* expression in other tissues such at the gut or limb. These results indicate that the population of *Ihh*-expressing prehypertrophic chondrocytes of the axial skeleton is affected in the *Bapx1* mutant mice.

Fgfr3 is the third member of the *Fgf* polypeptide growth factor receptor family. Point mutations in *Fgfr3* in mouse or human lead to retardation in bone growth, achondroplasia, reduced proliferation of cartilage and overall bone shortening (Cohen, 1998; Wilkie, 1997). The expression of *Fgfr3* was decreased in the vertebral bodies of the *Bapx1* null embryos, but *Fgfr3* expression was not affected in other tissues, like the neural tube, that do not express *Bapx1*. *Fgfr3* is believed to play a role in chondrocyte proliferation and the transition from proliferative to prehypertrophic chondrocytes (Colvin et al., 1996; Wang et al., 1999). *Bapx1* may be controlling the entry of certain prevertebral mesenchymal stem cells into the chondrogenic pathway and the loss of *Fgfr3* expression in the *Bapx1* null embryos is consistent with this. Bone morphogenetic protein 4, *Bmp4* is a member of the TGFβ super family of signaling proteins. The *Bmps* are homologues of *dpp* in *Drosophila*, and function via diffusion within the extracellular matrix and interact either with their cognate receptors or with antagonists such as *noggin* and *chordin* (reviewed in Graff, 1997; Hirsinger et al., 1998). In the mouse, *Bmp4* is expressed within the perichondrial region of both the axial and appendicular skeleton and its expression in the perichondrium appears to be under the negative control of the *Ihh* signaling pathway (Naski et al., 1998). In the *Bapx1* null embryos, the expression on *Bmp4* was altered such that it was no longer strictly confined to the perichondrial region, but instead had assumed a much more widespread and homogeneous domain of expression, with transcripts detectable throughout all the remaining cells of the vertebral body. Since *Ihh* was downregulated in the *Bapx1* null embryos, the upregulation of *Bmp4* in these same tissues is consistent with the proposed negative feedback control of *Ihh* (Naski et al., 1998), although a more direct effect of *Bapx1* on *Bmp4* regulation may also exist.

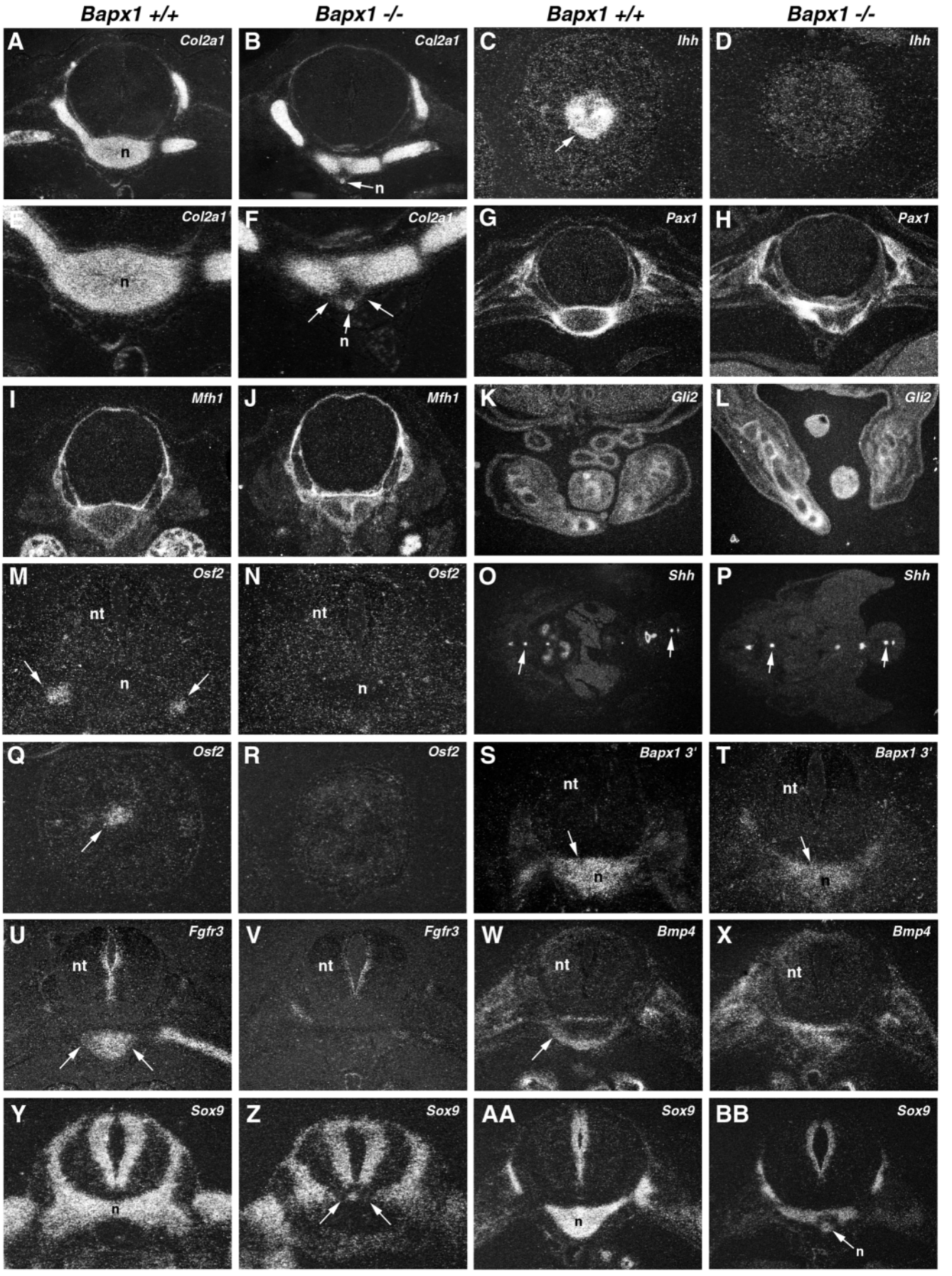
Bapx1 +/+
Bapx1 -/-
Bapx1 +/+
Bapx1 -/-
A Col2a1
B Col2a1
C Ihh
D Ihh
E Col2a1
F Col2a1
G Pax1
H Pax1
I Mfh1
J Mfh1
K Gli2
L Gli2
M Osf2
N Osf2
O Shh
P Shh
Q Osf2
R Osf2
S Bapx1 3'
T Bapx1 3'
U Fgfr3
V Fgfr3
W Bmp4
X Bmp4
Y Sox9
Z Sox9
AA Sox9
BB Sox9
n
nt

Fig. 6. RNA in situ analysis of gene expression in *Bapx1* wild-type and null embryos. Transverse sections through E14.5 (A-L,Q,R), E12.5 (M-P,S-X,AA,BB) and E10.5 (Y,Z) embryos. The *Bapx1* genotype is shown at the top of each column. The RNA in situ probe employed is indicated in the upper right corner of each panel. All sections are oriented with dorsal towards the top, except O,P which have dorsal to the left. Relative to wild-type embryos, *Bapx1* null embryos showed a reduction in the expression of *alpha 1(II) collagen* (*Col2a1*, A,B,E,F), *Indian hedgehog*, (*Ihh* C,D), *Osf2* (M,N,Q,R), *Fgfr3* (U,V) and *Sox9* (Y-BB) and in increase in *Bmp4* expression (W,X). For *alpha 1(II) collagen*, this effect was most pronounced in cells closest to the notochord (n), indicated by arrows in F. For *Fgfr3*, there was a loss of expression throughout all of the cells of the vertebral body, however, the expression in the adjacent neural tube was unaffected (U,V). For *Osf2*, strong reductions in expression were observed at E12.5 in the pedicles of the neural arches (arrows in M) and at E14.5 in the vertebral bodies of the caudal vertebrae (arrow in Q). A similar reduction in the level of expression was observed for *Ihh* (C,D). *Sox9* showed a reduction in expression similar to *alpha 1(II) collagen*, which was most pronounced in cells closest to the notochord (n, panels Y-BB) indicated by arrows in Z. Perturbations in transcript distribution were observed for *Pax1* and*Mfh1* (G,H,I,J). No significant changes were observed for either *Gli2* (K,L) or *Shh* (O,P) transcript levels or distribution. The *Bapx1 3′* probe (S,T) detects a portion of the *Bapx1* mRNA that is present in the *Bapx1* null allele. This probe marks *Bapx1* null cells that normally would express Bapx1 protein. A similar transcript distribution among the cells of the prevertebrae in the wild-type and *Bapx1* null embryos is observed (arrows in S,T), which indicates that there are no significant problems in cell migration or cell proliferation for cells which normally express *Bapx1* at E12.5 in the mutant embryos. Abbreviations: n, notochord; nt, neural tube.

The *Mfh1* gene encodes a winged helix/forkhead domain transcription factor, which is normally expressed in paraxial and presomitic mesoderm, in the developing somites and in condensing sclerotome (Iida et al., 1997; Winnier et al., 1997). *Mfh1* null mice have axial skeletal malformations in structures derived from cephalic and somitic mesoderm that are reminiscent of those observed in *Bapx1* null mice (Iida et al., 1997; Winnier et al., 1997). Interestingly, no significant reduction in the expression of *Mfh1* was observed in the *Bapx1* null embryos; however, in both types of mutant animals a reduction in *alpha 1 (II) collagen (Col2a1)* expression was observed, suggesting that both of these transcription factors likely lay upstream of *Col2a1*. *Sox9* is a high-mobility-group (HMG) domain transcription factor that is expressed in chondroblasts and other embryonic tissues and the onset of its expression in the embryo parallels the onset of *Col2a1* expression (Wright et al., 1995; Zhao et al., 1997). *Sox9* has also been shown to bind to critical elements in the *Col2a1* enhancer and can *trans*-activate the *Col2a1* enhancer in cell culture and transgenic animals and produce ectopic cartilage in vivo (Bell et al., 1997; Healy et al., 1999; Lefebvre et al., 1997; Ng et al., 1997). Embryonic stem cells that lack both copies of *Sox9* are incapable of colonizing the chondroblast lineage and are excluded from all cartilages (Bi et al., 1999) and humans with only one copy of *Sox9* suffer from campomelic dysplasia, a severe skeletal dysmorphology syndrome (OMIM 114290). In the *Bapx1* null embryos, *Sox9* expression is reduced in prechondroblasts of the sclerotome in early stage embryos and in cells of the ventral vertebral body in older embryos. The decrease in *Sox9* expression is consistent with a decrease in *Col2a1* expression in these same cells in the *Bapx1* null embryos, suggesting that the effect of *Bapx1* on *Col2a1* expression may be mediated via changes in *Sox9* expression levels.

Another transcription factor involved in sclerotome patterning is *Pax1*, which belongs to the paired box-containing gene family of transcription factors (Balling et al., 1996). The expression pattern of *Pax1* in the developing vertebral column is very similar to *Bapx1* at early stages where it is expressed in the presclerotome cells of the somite from E8.25 onward and then shows stronger expression in the caudal half of the somite by E10.5. The absence of vertebral bodies in the lumbar regions of the *Pax1* null mice is strikingly similar to that of *Bapx1* null animals. However, the morphological alterations in extravertebral components, like the sternum and the scapula, that are present in *Pax1* mutants are not present in *Bapx1* mutant mice. Overall the *Bapx1* axial skeletal defects are more severe than those observed in the *Pax1* null mice, as all of the vertebrae are dramatically affected in *Bapx1* mutants, as well as the mesoderm-derived bones of the skull.

Human *Bapx1* and redundant developmental function

The human homologue of *Bapx1* has been identified and mapped to 4p16.1 (Tribioli and Lufkin, 1997) although pathogenic mutations have not yet been identified in this gene in humans. In murine *Bapx1* null embryos, the skeletal defects are detectable at E12.5, this embryonic stage corresponds approximately to day 40 in humans. Based on the vertebral defects only, potentially the *Bapx1* null embryo phenotype could have a human counterpart in an autosomal recessive form of neonatal lethal spondylodysplasia. However, the absence of limb defects in the murine null mutants makes it difficult to recognize the corresponding human disease in the group of the skeletal disorders that have been mapped by linkage to 4p16.1. Only *Bapx1*-expressing cells are affected in *Bapx1* null mice, however, the morphological abnormalities are restricted to specific components of the axial skeleton and to the spleen. The concentration of skeletal defects in the *Bapx1* null animals primarily to cells surrounding the notochord suggests a possible interaction between these cells and potential factors secreted from the notochord, such as *Shh*. Whether *Bapx1* is regulated by *Shh* or whether other diffusible factors participate in the restriction of the *Bapx1* null phenotype remains to be determined. Another significant domain of expression of *Bapx1* in the developing embryo is the limbs (Tribioli et al., 1997; Tribioli and Lufkin, 1997), yet surprisingly, no obvious defect in limb morphogenesis or cellular differentiation was observed in the *Bapx1* null embryos. The lack of an effect of *Bapx1* may be the result of the expression of related *Bapx* family members that have yet to be identified (Sidow, 1996) or to a parallel regulatory network, which may functionally compensate for loss of *Bapx1* in certain tissues.

We would like to thank Rudi Balling, Brigid Hogan, Mitch Goldfarb, Peter Gruss, Alex Joyner, Gerard Karsenty, Peter Koopman, Andy McMahon and Francesco Ramirez for providing RNA in situ probes. Andras Nagy for providing the CMV-Cre transgenic mice, Benoit de Crombrugghe for the *mouse pro alpha 1(II) collagen-lacZ* plasmid, and David Neustaedter and Maria Nikolova for technical

assistance. The financial support of Telethon-Italy (Grant n.D.75) to C. T. is gratefully acknowledged.

REFERENCES

Andrikopoulos, K., Suzuki, H. R., Solursh, M. and Ramirez, F. (1992). Localization of *pro-alpha2 (V) collagen* transcripts in the tissues of the developing mouse embryo. *Dev. Dynamics* **195**, 113-120.

Aubin, J. E., Liu, F., Malaval, L. and Gupta, A. K. (1995). Osteoblast and chondroblast differentiation. *Bone* **17**, 77-83.

Azpiazu, N. and Frasch, M. (1993). *tinman and bagpipe:* two homeo box genes that determine cell fates in the dorsal mesoderm of *Drosophila*. *Genes Dev.* **7**, 1325-1340.

Azpiazu, N., Lawrence, P., Vincent, J.-P. and Frasch, M. (1996). Segmentation and specification of the *Drosophila* mesoderm. *Genes Dev.* **10**, 3183-3194.

Balling, R., Neubuser, A. and Christ, B. (1996). *Pax* genes and sclerotome development. *Semin. Cell Dev. Biol.* **7**, 129-136.

Bell, D. M., Leung, K. K., Wheatley, S. C., Ng, L. J., Zhou, S., Ling, K. W., Sham, M. H., Koopman, P., Tam, P. P. and Cheah, K. S. (1997). SOX9 directly regulates the type-II collagen gene. *Nature Genet.* **16**, 174-178.

Bi, W., Deng, J. M., Zhang, Z., Behringer, R. R. and de Crombrugghe, B. (1999). Sox9 is required for cartilage formation. *Nat. Genet.* **22**, 85-89.

Borycki, A. G., Mendham, L. and Emerson, C. P., Jr. (1998). Control of somite patterning by *Sonic hedgehog* and its downstream signal response genes. *Development* **125**, 777-790.

Cancedda, R., Descalzi Cancedda, F. and Castagnola, P. (1995). Chondrocyte differentiation. *Int. Rev. Cytol.* **159**, 265-358.

Cohen, M. M., Jr. (1998). Achondroplasia, hypochondroplasia and thanatophoric dysplasia: clinically related skeletal dysplasias that are also related at the molecular level. *Int. J. Oral Maxillofac. Surg.* **27**, 451-455.

Colvin, J. S., Bohne, B. A., Harding, G. W., McEwen, D. G. and Ornitz, D. M. (1996). Skeletal overgrowth and deafness in mice lacking fibroblast growth factor receptor 3. *Nat. Genet.* **12**, 390-397.

Couly, G. F., Coltey, P. M. and Le Douarin, N. M. (1992). The developmental fate of the cephalic mesoderm in quail-chick chimeras. *Development* **114**, 1-15.

Couly, G. F., Coltey, P. M. and Le Douarin, N. M. (1993). The triple origin of skull in higher vertebrates: a study in quail- chick chimeras. *Development* **117**, 409-429.

D'Mello, S. R. (1998). Molecular regulation of neuronal apoptosis. *Curr. Top. Dev. Biol.* **39**, 187-213.

Ducy, P., Zhang, R., Geoffroy, V., Ridall, A. L. and Karsenty, G. (1997). *Osf2/Cbfa1*: a transcriptional activator of osteoblast differentiation. *Cell* **89**, 747-754.

Echelard, Y., Epstein, D. J., St-Jacques, B., Shen, L., Mohler, J., McMahon, J. A. and McMahon, A. P. (1993). *Sonic hedgehog*, a member of a family of putative signaling molecules, is implicated in the regulation of CNS polarity. *Cell* **75**, 1417-1430.

Frasch, M., Chen, X. and Lufkin, T. (1995). Evolutionary-conserved enhancers direct region-specific expression of the murine *Hoxa-1* and *Hoxa-2* loci in both mice and *Drosophila*. *Development* **121**, 957-974.

Furumoto, T. A., Miura, N., Akasaka, T., Mizutani-Koseki, Y., Sudo, H., Fukuda, K., Maekawa, M., Yuasa, S., Fu, Y., Moriya, H. et al. (1999). Notochord-dependent expression of MFH1 and PAX1 cooperates to maintain the proliferation of sclerotome cells during the vertebral column development. *Dev. Biol.* **210**, 15-29.

Goldfarb, M. (1990). The fibroblast growth factor family. *Cell Growth & Differentiation* **1**, 439-445.

Graff, J. M. (1997). Embryonic patterning: To BMP or not to BMP, that is the question. *Cell* **89**, 171-174.

Green, M. C. (1967). A defect of the splanchnic mesoderm caused by the mutant gene dominant hemimelia in the mouse. *Dev. Biol.* **15**, 62-89.

Hanken, J. and Thorogood, P. (1993). Evolution and development of the vertebrate skull: The role of pattern formation. *Trends in Ecology and Evolution* **8**, 9-14.

Healy, C., Uwanogho, D. and Sharpe, P. T. (1999). Regulation and role of Sox9 in cartilage formation. *Dev. Dyn.* **215**, 69-78.

Hirsinger, E., Jouve, C., Malapert, P. and Pourquie, O. (1998). Role of growth factors in shaping the developing somite. *Mol. Cell. Endocrinol.* **140**, 83-87.

Iida, K., Koseki, H., Kakinuma, H., Kato, N., Mizutani-Koseki, Y., Ohuchi, H., Yoshioka, H., Noji, S., Kawamura, K., Kataoka, Y. et al. (1997). Essential roles of the winged helix transcription factor MFH-1 in aortic arch patterning and skeletogenesis. *Development* **124**, 4627-4638.

Johnson, R. L., Laufer, E., Riddle, R. D. and Tabin, C. (1994). Ectopic expression of *sonic hedgehog* alters dorsal-ventral patterning of somites. *Cell* **79**, 1165-1173.

Komori, T., Yagi, H., Nomura, S., Yamaguchi, A., Sasaki, K., Deguchi, K., Shimizu, Y., Bronson, R. T., Gao, Y. H., Inada, M. et al. (1997). Targeted disruption of *Cbfa1* results in a complete lack of bone formation owing to maturational arrest of osteoblasts. *Cell* **89**, 755-764.

Koseki, H., Wallin, J., Witing, J., Mizutani, Y., Kispert, A., Ebensperger, C., Herrmann, B. G., Christ, B. and Balling, R. (1993). A role for *Pax-1* as a mediator of notochordal signals during the dorsoventral specification of vertebrae. *Development* **119**, 649-660.

Lanske, B., Karaplis, A. C., Lee, K., Luz, A., Vortkamp, A., Pirro, A., Karperien, M., Defize, L. H. K., Ho, C., Mulligan, R. C. et al. (1996). *PTH/PTHrP* receptor in early development and *Indian hedgehog*-regulated bone growth. *Science* **273**, 663-666.

Lassar, A. B. and Munsterberg, A. E. (1996). The role of positive and negative signals in somite patterning. *Curr. Opin. Neurobiol.* **6**, 57-63.

Lefebvre, V., Huang, W. D., Harley, V. R., Goodfellow, P. N. and deCrombrugghe, B. (1997). SOX9 is a potent activator of the chondrocyte-specific enhancer of the pro alpha 1(II) collagen gene. *Mol. Cell. Biol.* **17**, 2336-2346.

Li, X., Wang, W. and Lufkin, T. (1997). Dicistronic *lacZ* and alkaline phosphatase reporter constructs permit simultaneous histological analysis of expression from multiple transgenes. *BioTechniques* **23**, 874-882.

Liu, L., Khastgir, A., McCauley, J. M., Dunn, S. T., Morrissey, J. H., Christakos, S., Hughes, M. R. and Bourdeau, J. E. (1996). RT-PCR microlocalization of mRNAs for calbindin D28k and vitamin D receptor in the murine nephron. *Am. J. Physiol.* **270**, F677-F681.

Lufkin, T., Lohnes, D., Mark, M., Dierich, A., Gorry, P., Gaub, M. P., LeMeur, M. and Chambon, P. (1993). High postnatal lethality and testis degeneration in retinoic acid receptor alpha mutant mice. *Proc. Natl. Acad. Sci. USA* **90**, 7225-7229.

Lufkin, T., Mark, M., Hart, C. P., LeMeur, M. and Chambon, P. (1992). Homeotic transformation of the occipital bones of the skull by ectopic expression of a homeobox gene. *Nature* **359**, 835-841.

Lyons, K. M., Pelton, R. W. and Hogan, B. L. (1989). Patterns of expression of murine Vgr-1 and BMP-2a RNA suggest that transforming growth factor-β-like genes coordinately regulate aspects of embryonic development. *Genes Dev.* **3**, 1657-1668.

Metsaranta, M., Garofalo, S., Smith, C., Niederreither, K., de Crombrugghe, B. and Vuorio, E. (1995). Developmental expression of a type II collagen/β-galactosidase fusion gene in transgenic mice. *Dev. Dyn.* **204**, 202-210.

Milligan, C. E. and Schwartz, L. M. (1997). Programmed cell death during animal development. *Brit. Med. Bull.* **53**, 570-590.

Nagy, A., Moens, C., Ivanyi, E., Pawling, J., Gertsenstein, M., Hadjantonakis, A. K., Pirity, M. and Rossant, J. (1998). Dissecting the role of *N-myc* in development using a single targeting vector to generate a series of alleles. *Curr. Biol.* **8**, 661-664.

Naski, M. C., Colvin, J. S., Coffin, J. D. and Ornitz, D. M. (1998). Repression of hedgehog signaling and BMP4 expression in growth plate cartilage by fibroblast growth factor receptor 3. *Development* **125**, 4977-4988.

Ng, L. J., Wheatley, S., Muscat, G. E. O., ConwayCampbell, J., Bowles, J., Wright, E., Bell, D. M., Tam, P. P. L., Cheah, K. S. E. and Koopman, P. (1997). SOX9 binds DNA, activates transcription, and coexpresses with type II collagen during chondrogenesis in the mouse. *Dev. Biol.* **183**, 108-121.

Noden, D. M. (1992). Vertebrate craniofacial development: novel approaches and new dilemmas. *Curr. Opin. Genet. Dev.* **2**, 576-581.

Otto, F., Thornell, A. P., Crompton, T., Denzel, A., Gilmour, K. C., Rosewell, I. R., Stamp, G. W., Beddington, R. S., Mundlos, S., Olsen, B. R. et al. (1997). *Cbfa1*, a candidate gene for cleidocranial dysplasia syndrome, is essential for osteoblast differentiation and bone development. *Cell* **89**, 765-771.

Pourquie, O., Fan, C. M., Coltey, M., Hirsinger, E., Watanabe, Y., Breant, C., Francis-west, P., Brickell, P., Tessier Lavigne, M. and Ledouarin, N. M. (1996). Lateral and axial signals involved in avian somite patterning: a role for BMP4. *Cell* **84**, 461-471.

Sanders, E. J. and Wride, M. A. (1995). Programmed cell death in development. *Int. Rev. Cytol.* **163**, 105-173.

Sheehan, D. C. and Hrapchak, B. B. (1987). *Theory and Practice of Histotechnology.* Columbus: Battelle Press.

Sidow, A. (1996). Gen(om)e duplications in the evolution of vertebrates. *Curr. Opin. Gen. Dev.* **6**, 715-722.

Tiret, L., LeMouellic, H., Maury, M. and Brulet, P. (1998). Increased apoptosis of motoneurons and altered somatotopic maps in the brachial spinal cord of *Hoxc-8*-deficient mice. *Development* **125**, 279-291.

Tribioli, C., Frasch, M. and Lufkin, T. (1997). *Bapx1:* an evolutionary-conserved homologue of the *Drosophila bagpipe* homeobox gene is expressed in splanchnic mesoderm and the embryonic skeleton. *Mech. Dev.* **65**, 145-162.

Tribioli, C. and Lufkin, T. (1997). Molecular cloning, chromosomal mapping and developmental expression of *BAPX1*, a novel human homeobox-containing gene homologous to *Drosophila bagpipe*. *Gene* **203**, 225-233.

Vortkamp, A., Lee, K., Lanske, B., Segre, G. V., Kronenberg, H. M. and Tabin, C. J. (1996). Regulation of rate of cartilage differentiation by indian hedgehog and PTH-related protein. *Science* **273**, 613-622.

Vortkamp, A., Pathi, S., Peretti, G. M., Caruso, E. M., Zaleske, D. J. and Tabin, C. J. (1998). Recapitulation of signals regulating embryonic bone formation during postnatal growth and in fracture repair. *Mech. Dev.* **71**, 65-76.

Wang, W., VandeWater, T. and Lufkin, T. (1998). Inner ear and maternal reproductive defects in mice lacking the *Hmx3* homeobox gene. *Development* **125**, 621-634.

Wang, Y., Spatz, M. K., Kannan, K., Hayk, H., Avivi, A., Gorivodsky, M., Pines, M., Yayon, A., Lonai, P. and Givol, D. (1999). A mouse model for achondroplasia produced by targeting fibroblast growth factor receptor 3. *Proc. Natl Acad. Sci. USA* **96**, 4455-4460.

Wilkie, A. O. (1997). Craniosynostosis: genes and mechanisms. *Hum. Mol. Genet.* **6**, 1647-1656.

Wilm, B., Dahl, E., Peters, H., Balling, R. and Imai, K. (1998). Targeted disruption of *Pax1* defines its null phenotype and proves haploinsufficiency. *Proc. Natl Acad. Sci. USA* **95**, 8692-8697.

Winnier, G. E., Hargett, L. and Hogan, B. L. M. (1997). The winged helix transcription factor *MFH1* is required for proliferation and patterning of paraxial mesoderm in the mouse embryo. *Gene Dev.* **11**, 926-940.

Wright, E., Hargrave, M. R., Christiansen, J., Cooper, L., Kun, J., Evans, T., Gangadharan, U., Greenfield, A. and Koopman, P. (1995). The *Sry*-related gene *Sox*-9 is expressed during chondrogenesis in mouse embryos. *Nat. Genet.* **9**, 15-20.

Yang, Y., Guillot, P., Boyd, Y., Lyon, M. F. and McMahon, A. P. (1998). Evidence that preaxial polydactyly in the Doublefoot mutant is due to ectopic Indian Hedgehog signaling. *Development* **125**, 3123-3132.

Zhao, Q., Eberspaecher, H., Lefebvre, V. and De Crombrugghe, B. (1997). Parallel expression of Sox9 and Col2a1 in cells undergoing chondrogenesis. *Dev. Dyn.* **209**, 377-386.

Zhou, G., Garofalo, S., Mukhopadhyay, K., Lefebvre, V., Smith, C. N., Eberspaecher, H. and De Crombrugghe, B. (1995). A 182 bp fragment of the mouse *pro alpha 1(II) collagen* gene is sufficient to direct chondrocyte expression in transgenic mice. *J. Cell Sci.* **108**, 3677-3684.